



## RESEARCH ARTICLE

# Electron Detachment Dissociation of Underivatized Chloride-Adducted Oligosaccharides

James R. Kornacki,<sup>1,2</sup> Julie T. Adamson,<sup>1,3</sup> Kristina Håkansson<sup>1</sup><sup>1</sup>Department of Chemistry, University of Michigan, 930 North University Ave., Ann Arbor, MI 48109, USA<sup>2</sup>Present Address: Department of Chemistry, Northwestern University, 2145 Sheridan Road, Evanston, IL 60208-3113, USA<sup>3</sup>Present Address: Millennium Pharmaceuticals, Cambridge, MA 02139, USA

## Abstract

Chloride anion attachment has previously been shown to aid determination of saccharide anomeric configuration and generation of linkage information in negative ion post-source decay MALDI tandem mass spectrometry. Here, we employ electron detachment dissociation (EDD) and collision activated dissociation (CAD) for the structural characterization of underivatized oligosaccharides bearing a chloride ion adduct. Both neutral and sialylated oligosaccharides are examined, including maltoheptaose, an asialo biantennary glycan (NA2), disialylacto-*N*-tetraose (DSLNT), and two LS tetrasaccharides (LSTa and LSTb). Gas-phase chloride-adducted species are generated by negative ion mode electrospray ionization. EDD and CAD spectra of chloride-adducted oligosaccharides are compared to the corresponding spectra for doubly deprotonated species not containing a chloride anion to assess the role of chloride adduction in the stimulation of alternative fragmentation pathways and altered charge locations allowing detection of additional product ions. In all cases, EDD of singly chloridated and singly deprotonated species resulted in an increase in observed cross-ring cleavages, which are essential to providing saccharide linkage information. Glycosidic cleavages also increased in EDD of chloride-adducted oligosaccharides to reveal complementary structural information compared to traditional (non-chloride-assisted) EDD and CAD. Results indicate that chloride adduction is of interest in alternative anion activation methods such as EDD for oligosaccharide structural characterization.

**Key words:** MS/MS, Tandem mass spectrometry, CAD collision activated dissociation, EDD electron detachment dissociation, FT-ICR Fourier transform ion cyclotron resonance, Carbohydrate, Structural characterization, Oligosaccharide, Chloride adduct

## Introduction

Interest in glycomics, the study of biological carbohydrates (or saccharides), continues to grow as the importance of glycoconjugates is realized. Glycoconjugates are oligosaccharide (or glycan)-containing biomolecules whose activity has been linked to a variety of important biological functions [1, 2], such as protein folding [3] and immune system response [4]. The role of glycoconjugates as crucial cellular

mediators is increasingly apparent as glycosylation is one of the most prevalent post-translational modifications. Variety among oligosaccharide structures and isomeric forms may play a significant role for the biological function of glycoconjugates, and an understanding of the structural complexities of these compounds is a necessary first step in fully realizing their function. Oligosaccharides contain many diverse features and complete structural characterization requires information regarding linkage, sequence, branching, and anomeric configuration (a term defining the stereochemistry of the glycosidic bond).

Correspondence to: Kristina Håkansson; e-mail: kicki@umich.edu

Received: 19 June 2011  
Revised: 22 July 2012  
Accepted: 23 July 2012  
Published Online: 22 August 2012

Mass spectrometry is widely employed for the structural characterization of oligosaccharides due to its high sensitivity, minimal sample consumption, and relatively short acquisition times. Instruments that allow for tandem mass spectrometry (MS/MS or MS<sup>n</sup>) have emerged as indispensable tools for oligosaccharide structural analysis [5–7], particularly when allowing for multiple stages of MS/MS. Fourier transform ion cyclotron resonance mass spectrometry (FT-ICR MS) offers the advantage of several MS/MS techniques combined with high mass accuracy and resolution. Tandem MS of oligosaccharides generally produces glycosidic and cross-ring product ions, both of which reveal important information regarding structure. Glycosidic cleavages occur between monosaccharide units and indicate saccharide sequence and branching while cross-ring cleavages provide information regarding saccharide linkage and are particularly useful when occurring at branching residues. Several factors affect the extent of fragmentation and the types of product ions detected, including the ionization technique, the lifetime of the ion before detection, and the amount of energy deposited into the ion. The presence of functional groups also affects fragmentation, and Zaia and coworkers have shown that sialylated oligosaccharides (those containing a sialic acid residue) require more energy to induce fragmentation than their asialo or nitrate-adducted counterparts in collision activated dissociation (CAD) [8].

Most modern mass analyzers rely upon low energy CAD for MS/MS experiments. Low energy activation methods typically generate glycosidic bond cleavages when applied to oligosaccharide analysis. However, it has been shown that oligosaccharides adducted with alkali, alkaline earth, and transition metals often yield more cross-ring product ions than the corresponding protonated species following vibrational excitation methods such as CAD and infrared multiphoton dissociation (IRMPD) [9–13]. More recently, vibrational activation has been used in conjunction with electron capture dissociation (ECD) [14, 15] for positive ion mode oligosaccharide analysis [13, 16]. ECD occurs via radical-driven fragmentation pathways when polycationic molecules are irradiated with low-energy electrons (~1 eV) and generates charge-reduced radical species and product ions. ECD has been widely used for peptide and protein cation characterization [17] because it regularly leaves labile modifications intact while provoking extensive backbone fragmentation [18–23]. Previous work from our lab demonstrated that oligosaccharides adducted with divalent metal cations exhibit highly complementary fragmentation in ECD compared to IRMPD [13]. Han and Costello have recently shown that electron transfer dissociation (ETD) in combination with CAD is also valuable for characterization of permethylated oligosaccharides [24]. However, permethylation does involve additional wet chemistry, can be challenging for small sample amounts, and is not compatible with, e.g., sulfonated glycans such as glycosaminoglycans [GAGs].

Fewer studies regarding the analysis of oligosaccharides in negative ion mode mass spectrometry are available, but it is known that differences in fragmentation are observed

between oligosaccharide anions and cations [25–28]. Following CAD, anionic oligosaccharides tend to produce mostly C-type glycosidic and A-type cross-ring product ions while cationic species produce mostly B and Y-type glycosidic product ions (Domon and Costello nomenclature) [29]. Electron detachment dissociation (EDD) is a negative ion mode ion-electron reaction MS/MS technique typically showing lower fragmentation efficiency than ECD/ETD and requiring longer ion-electron interaction times (~1 s). Nevertheless, rich fragmentation chemistry occurs in EDD, frequently providing unique structural information for oligosaccharides, including GAGs [30–33]. Unlike ECD, EDD is used for the fragmentation of polyanions in negative ion mode [34]. Introduced in 2001, EDD relies upon radical formation from electron detachment and subsequent fragmentation of an originally polyanionic species when irradiated with medium-energy electrons (>10 eV). In addition to oligosaccharides, EDD has been applied to peptides [34–37], oligonucleotides [38, 39], and gangliosides [40]. Negative ion mode analysis is particularly amenable to acidic oligosaccharides as such compounds readily deprotonate. In addition, the tendency of sialylated oligosaccharides to lose sialic acid residues is not as apparent in negative compared to positive ion mode [41]. Furthermore, solvent background is typically lower in negative ion mode. We have previously shown a significant increase in A- and X-type cross-ring fragments following EDD of neutral and sialylated oligosaccharides that are not observed by vibrational excitation techniques [30].

Chloride anion attachment to analyze carbohydrates was first demonstrated by Harvey for N-linked glycans [42] and later used by Cole and co-workers to examine post-source decay of neutral and acidic oligosaccharides for determination of anomeric configurations [43]. Noting the ease at which neutral oligosaccharides form  $[M + \text{anion}]^-$  adducts, anion attachment was implemented to simultaneously analyze neutral and acidic carbohydrates without switching the instrument polarity. Here, we examine EDD of underivatized chloride-adducted oligosaccharides. The current study focuses on the fragmentation patterns of neutral and sialylated oligosaccharides and compares these fragmentation patterns to those obtained following EDD of doubly deprotonated species and CAD of chloride-adducted species.

## Experimental

### Sample Preparation

Maltoheptaose (Sigma-Aldrich, St. Louis, MO, USA), LS-tetrasaccharides (LSTa and LSTb), and an asialo biantennary glycan (NA2; V-Labs, Covington, LA, USA) were prepared in a solution of 50 % methanol (Fisher, Fair Lawn, NJ, USA) and 0.1 % ammonium hydroxide (Sigma) to a final concentration of 3  $\mu\text{M}$ . Chloride-adducted samples were prepared in a solution of 50 % methanol with ammonium chloride (Sigma-Aldrich) added to a final concentration of

21  $\mu\text{M}$ . Samples were refrigerated and undisturbed for at least 1 week.

### Mass Spectrometry

All experiments were performed with a 7-T FT-ICR mass spectrometer with a quadrupole front end (APEX-Q, Bruker Daltonics, Billerica, MA, USA) [44]. Oligosaccharide solutions were infused via an external Apollo II electrospray ion source at a flow rate of 60  $\mu\text{L}/\text{h}$  with the assistance of  $\text{N}_2$  nebulizing gas. The off-axis sprayer was grounded and the inlet capillary was set to approximately 2.5–3.1 kV for generation of oligosaccharide anions.  $\text{N}_2$  drying gas, 175  $^\circ\text{C}$ , was applied to assist desolvation of the ESI droplets. Following ion accumulation in the first hexapole for 50 ms, ions were mass selectively accumulated in the second hexapole for 2–6 s. Ions were then transferred through high-voltage ion optics and captured with dynamic trapping in an Infinity ICR cell [45]. The experimental sequence leading to the ICR cell fill was looped 4–8 times to achieve maximum precursor ion signal for EDD. Precursor ions were further isolated in the ICR cell using correlated harmonic excitation fields (CHEF) [46]. An indirectly heated hollow dispenser cathode [47] was used to perform EDD with a constant heating current of 2.0 A and a pulsed cathode bias voltage that varied between –20 and –35 V for 1–2 s. A 6 mm diameter lens electrode located immediately in front of the cathode was held 0.4–1.0 V higher than the bias voltage to regulate the number of electrons entering the ICR cell [44]. External CAD was performed in a hexapole following mass selective ion accumulation with argon as collision gas.

### Data Analysis

All spectra were acquired with XMASS software (Bruker Daltonics) in broadband mode from  $m/z$  200–2,000 using 256 k data points and summed over 20 or 50 scans for CAD or EDD experiments, respectively. Data processing was performed with MIDAS software [48]. A Hanning window function was applied, and the time-domain data were zero filled once prior to fast Fourier transformation followed by magnitude calculation. A peak list was generated and exported to Microsoft Excel for internal frequency-to-mass calibration with a two-term calibration equation. The calculated masses of the precursor ion and an abundant product ion were used for calibration. A second set of abundant ions at different ends of the spectrum were often used for confirmation of the calibration. Only assignments better than 20 ppm were included. This relatively high tolerance was needed due to the deterioration of mass accuracy as a result of the high space charge conditions during EDD causing increased ion magnetron motion. Product ion spectra were interpreted with the aid of the web application GlycoFragment (<http://www.glycosciences.de/tools/GlycoFragments/>) [49].

## Results and Discussion

All product ions are labeled according to the Domon and Costello nomenclature [29], where A-, B-, and C-type fragments contain the non-reducing end of the molecule, and X-, Y-, and Z-type fragments contain the reducing end. B-, C-, Y-, and Z-type ions arise from cleavage of glycosidic bonds, whereas A- and X-type ions result from cross-ring cleavages. When more than one product ion assignment is possible, alternative assignments are indicated in parentheses (e.g.,  $\text{C}_4(\text{Y}_4)$ ). Product ions arising from multiple cleavage sites are designated with a slash between the sites of cleavage (e.g.,  $\text{C}_2/\text{Z}_{3\beta} - 2\text{H}$ ). Letters  $\alpha$  and  $\beta$  are used to identify branched oligosaccharides where  $\alpha$  indicates the heavier branch. Product ions bearing a chloride anion as a charge carrier are denoted with a superscript Cl (e.g.,  $\text{C}_4^{\text{Cl}}$ ).

Two chloride-adducted neutral oligosaccharides were subjected to MS/MS by EDD and CAD to examine the fragmentation behavior of oligosaccharides lacking an acidic moiety. These two oligosaccharides included maltoheptaose, a linear oligosaccharide containing seven,  $\alpha 1 \rightarrow 4$  linked glucose units, and NA2, an asialo, biantennary glycan with the following composition:  $\text{Gal}\beta 4\text{GlcNAc}\beta 2\text{Man}\alpha 6$  ( $\text{Gal}\beta 4\text{GlcNAc}\beta 2\text{Man}\alpha 3$ ) $\text{Man}\beta 4\text{GlcNAc}\beta 4\text{GlcNAc}$  ( $\alpha$  or  $\beta$  indicates stereochemistry and the numbers indicate anomeric linkage to that particular carbon in the adjacent ring). EDD and CAD spectra from these singly chloridated oligosaccharides were compared to previously obtained spectra of doubly deprotonated samples [30].

### CAD and EDD of Chloridated Maltoheptaose

The EDD spectrum of singly deprotonated and singly chloridated maltoheptaose,  $[\text{M} - \text{H} + \text{Cl}]^{2-}$  (Figure 1a), shows extensive fragmentation resulting in only singly charged products, while CAD gave rise to singly and doubly charged product ions (Figure 1b). In most cases, peak assignments are ambiguous due to the symmetry of maltoheptaose which could theoretically produce B and Z, C and Y, as well as A and X-type fragments of identical masses. Differentiation of such ambiguous fragments can be achieved via reduction or  $^{18}\text{O}$  labeling [24]; however such strategies were not pursued to allow for a direct comparison with our previous work on doubly deprotonated oligosaccharides [30].

Although most product ions are even-electron species, some odd-electron products are observed following EDD through neutral hydrogen loss from the even-electron product. Ions exhibiting hydrogen loss typically form via a minor fragmentation pathway and are therefore of lower abundance than their even-electron counterparts. One exception is the ion at  $m/z$  646.2, denoted  $\text{B}_4(\text{Z}_4) - \text{H}$ , where the radical species is more abundant than the corresponding even-electron species. Identical behavior was seen in our previous work on EDD of doubly deprotonated maltoheptaose [30] and loss of neutral hydrogen from B-type ions has

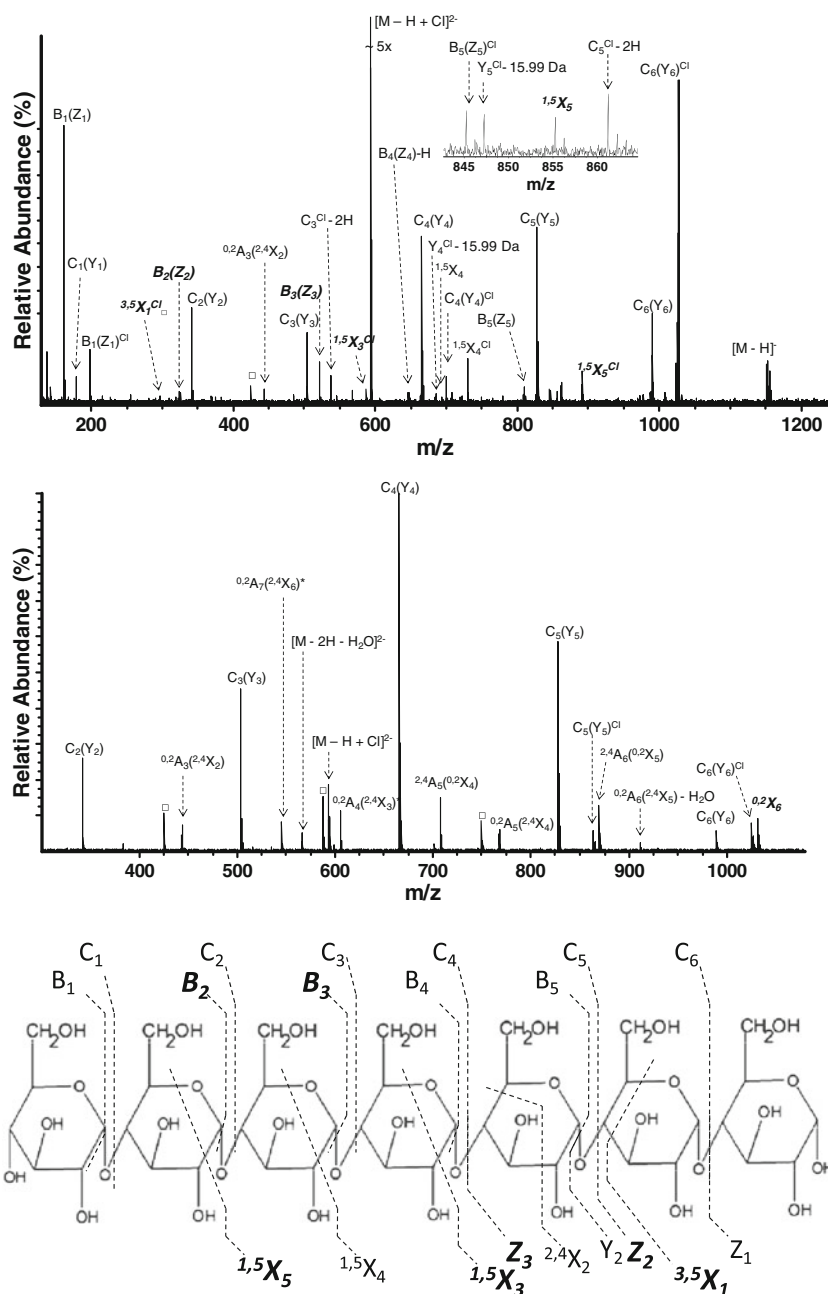


**Figure 1.** FT-ICR tandem mass spectra of deprotonated and chloridated maltoheptaose,  $[M - H + Cl]^{2-}$ : (top) EDD (50 scans, 2 s, bias voltage of  $-30$  V); (middle) CAD (30 scans, collision cell voltage 10 V). Product ions shown in bold are unique to the chloride-adducted species compared to the corresponding doubly deprotonated species. Squares indicate water loss from an adjacent product ion. Due to the symmetry of the molecule, several product ions cannot be unambiguously assigned (indicated by parentheses in the labels in each spectrum). Superscript Cl indicates product ions bearing a chloride anion; (bottom) fragmentation pattern observed following EDD of deprotonated and chloridated maltoheptaose

been reported by Amster and coworkers in EDD of GAGs [31]. Here, the addition of chloride to the precursor ion does not appear to alter the reproducibility of this fragment, indicating that electron detachment occurs from the deprotonated site rather than from the chloride adduct. This preference in electron detachment site may be rationalized based on the much higher electron affinity of a chlorine atom radical (3.61 eV [50]) compared with an alkoxide

radical (e.g., 1.7 eV for cyclobutoxide [51]) although these numbers are distant approximations in the molecular context of the oligosaccharide. The negative charge on this fragment may be due to neutral HCl loss from excess vibrational energy in EDD.

Further hydrogen loss is observed for two other product ions, occurring at  $m/z$  537.1 and 861.2 and denoted by  $C_3(Y_3)^{Cl} - 2H$  and  $C_5(Y_5)^{Cl} - 2H$ , respectively where the

loss of two neutral hydrogen atoms is the dominant pathway. (C – 2H)-type product ions have been observed by several investigators following high-energy CAD (heCAD) [52–56], by us in EDD of sialylated oligosaccharides [30], and by Amster and co-workers in EDD of GAGs [31–33]. However, these product ions were not observed following EDD of doubly deprotonated maltoheptaose [30]. In the current experiments, both these singly charged product ions bear a chloride anion, which likely explains their absence from EDD of doubly deprotonated maltoheptaose.

Two chloride-adducted product ions, denoted  $Z_5^{\text{Cl}} + 2\text{H}$  ( $m/z=847.2$ ) and  $Z_4^{\text{Cl}} + 2\text{H}$  ( $m/z=685.2$ ), which could alternatively correspond to  $Y_5^{\text{Cl}} - 16$  Da and  $Y_4^{\text{Cl}} - 16$  Da, were observed following EDD of chloride-adducted maltoheptaose. Previous work suggests that these products correspond to Z + 2H rather than the Y – 16 Da fragments reported by Kováčik et al. [57] and by Harvey et al. [52] from positive-ion mode heCAD. Hydrogen addition and abstraction has been observed following ECD of peptides [58, 59] and further documented for EDD of peptides [34]. Further support for the formation of (Z + 2H)-type ions, rather than (Y – 16)-type products, is shown in Figure 1a by the presence of complementary C – 2H species. For example, the products  $Z_4^{\text{Cl}} + 2\text{H}$  and  $C_3^{\text{Cl}} - 2\text{H}$  are complementary and together account for the intact mass of maltoheptaose. Chloride adduction appears to increase the likelihood of detecting complementary product ions. Such complementary product ion pairs are highly valuable in structural characterization studies.

Several unique cross-ring cleavages (not observed following CAD or IRMPD) were reported from EDD of doubly deprotonated maltoheptaose [30]. EDD of chloridated and singly deprotonated maltoheptaose,  $[M - \text{H} + \text{Cl}]^{2-}$ , shows several additional glycosidic and cross-ring fragments not observed by CAD or IRMPD, including  $B_2(Z_2)$ ,  $B_3(Z_3)$ ,  $^{3,5}X_1^{\text{Cl}}$ ,  $^{1,5}X_3^{\text{Cl}}$ , and  $^{1,5}X_5^{\text{Cl}}$ . X-type fragments are of particular interest since they are rarely observed following low energy CAD, IRMPD, or ECD of underivatized glycans although  $^{1,5}X$  ions do not provide linkage information. Here, the chloride anion is the major charge carrier for all X-type fragments. However, chloride adduction is not prerequisite to the detection of unique cross-ring fragments; for example, the singly charged  $^{1,5}X_5$  product ion exists in deprotonated ( $m/z$  855.3) as well as chloride-adducted states ( $m/z$  891.2). Again, the deprotonated fragment may be explained via neutral HCl loss.

For comparison, chloride-adducted maltoheptaose was subjected to CAD. Fragmentation of the chloride-adducted oligosaccharide (Figure 1b) is similar to the fragmentation of the doubly deprotonated oligosaccharide [30]. Both CAD spectra consist primarily of similar C- and A-type fragments. Previous studies of nitrate-adducted asialo N-linked and high mannose type glycans showed improved negative ion mode precursor ion abundance, higher resistance to in-source fragmentation, and production of similar C- and A-type product ions compared to deprotonated species [60, 61]. A

unique  $^{0,2}X_6$  ion is observed for the chloridated oligosaccharide even though it does not bear a chloride anion as charge carrier. With the exception of the peaks denoted  $C_6(Y_6)^{\text{Cl}}$  and  $C_5(Y_5)^{\text{Cl}}$ , no product ions contained a chloride anion. Such behavior suggests a labile interaction between the chloride anion and the deprotonated oligosaccharide that is easily disrupted upon collisional activation and may explain why only one unique product ion was observed in CAD of the chloride-adducted species.

### *EDD and CAD of a Chloride-Adducted Asialo Biantennary Glycan (NA2)*

EDD and CAD spectra were collected for an asialo biantennary glycan (NA2) bearing either one or two chloride anions to form the doubly charged precursor ion. Unlike maltoheptaose,  $[M + 2\text{Cl}]^{2-}$  was significantly more abundant following ESI than the  $[M - \text{H} + \text{Cl}]^{2-}$  species, which may be due to NA2's increased size. For the sake of consistency, only the  $[M - \text{H} + \text{Cl}]^{2-}$  precursor is further discussed.

EDD of singly deprotonated NA2 bearing a chloride adduct resulted in a combination of singly and doubly charged product ions (denoted with an asterisk; Figure 2a), matching observations from EDD of the doubly deprotonated precursor [30]. Many of the doubly charged products could not be identified and likely arise from direct decomposition of the activated precursor ion rather than resulting from radical formation and subsequent fragmentation. All product ions appear to be even-electron species since neutral loss of a hydrogen atom was not observed as a dominant fragmentation pathway. However, the observation of  $C_4^{\text{Cl}} - 2\text{H}$  and  $C_5^{\text{Cl}} - 2\text{H}$  products, at  $m/z=1267.4$  and 1470.5, respectively, lends further evidence to the chloride anion's role in the detection of unique fragments, not observed following EDD of doubly deprotonated NA2 [30]. Also observed are products resulting from multiple cleavage sites, such as  $^{2,4}A_6/Y_4$ , but such products are not exclusively observed for the chloride-adducted precursor. Neither is one of the most abundant product ions, which corresponds to the loss of the 3-linked antenna and two reducing GlcNAc residues (labeled GlcNAcMan<sub>3</sub> – H<sub>2</sub>O at  $m/z=688.2$ ). Yet, the reproducibility of this product ion is important as its location at the oligosaccharide's branch point allows for determination of the monosaccharide composition for the 6-linked and the 3-linked antennae.

Several unique cross-ring cleavages and a previously unobserved  $B_1$  ion were noted following EDD of the chloride-adducted oligosaccharide, including  $^{0,2}A_2$ ,  $^{1,3}A_3$ ,  $^{0,2}A_4$ ,  $^{2,4}A_6^{\text{Cl}}$ ,  $^{1,5}X_4^{\text{Cl}}$ , and  $^{1,5}X_5^{\text{Cl}}$ . The mechanism yielding  $^{0,2}A$ -type ions from CAD is generally accepted to involve anomeric ring opening followed by retro-aldol rearrangement by the hydroxyl group in the 3-position [62–65]. Because a free OH group in the 3 position is required for such rearrangement, the absence of  $^{0,2}A$ -type ions for 3-linked residues has been used to justify this mechanism. Here, we observe a  $^{0,2}A$ -type ion ( $^{0,2}A_4$ ) at the 3-linked

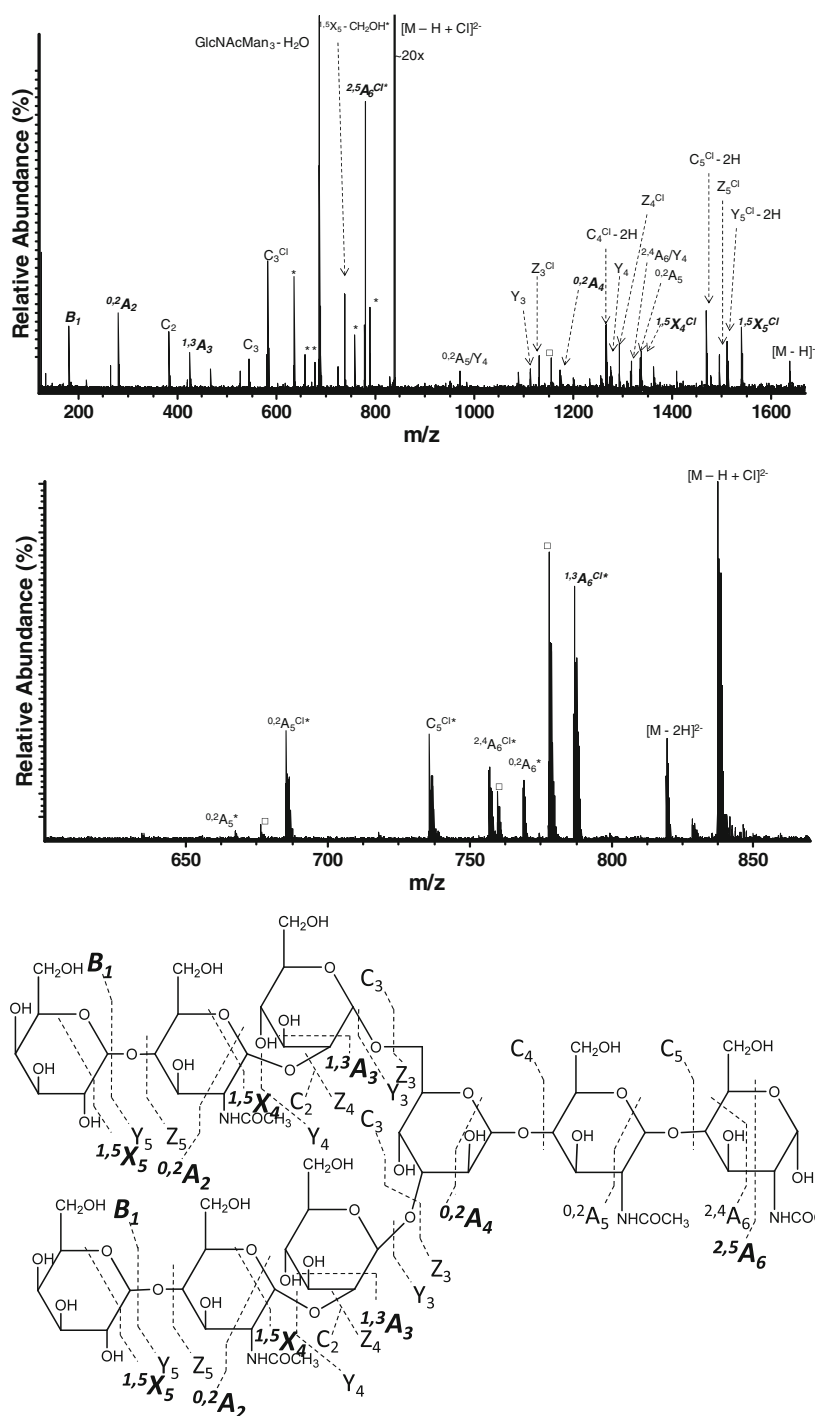


**Figure 2.** FT-ICR tandem mass spectra of a deprotonated and chloridated asialo, biantennary glycan (NA2),  $[M - H + Cl]^{2-}$ : (top) EDD (50 scans, 2 s, bias voltage of  $-25$  V); (middle) CAD (30 scans, collision cell voltage 4 V). Product ions shown in bold are unique to the chloride-adducted species compared to the corresponding doubly deprotonated species. Doubly charged product ions are indicated with an asterisk next to a product ion assignment. Squares indicate water loss from an adjacent product ion. Superscript Cl indicates product ions bearing a chloride anion; (bottom) fragmentation pattern observed following EDD of a deprotonated and chloride-adducted asialo, biantennary glycan (NA2)

mannose residue, suggesting that formation of this ion in EDD results from secondary decomposition of a  $Y_3$  ion, or by a radical-driven mechanism that is not yet understood. Finally, the presence of a chloride anion on various products

can indicate the location(s) of anion interaction. X-type product ions, hydrogen abstracted C-type ions, and the  $^{2,5}A_6^{Cl}$  ion all include chloride as charge carrier, suggesting that the anion interacts near the middle of the gas phase NA2

molecule, or that a mixture of charge isomers exists in the gas phase.

CAD of chloridated NA2 showed similar results to maltoheptaose with dissociation yielding only doubly charged C- and A-type fragments (Figure 2b). Although fragmentation was minimal following relatively low energy collisions, a high abundance  $^{0,2}A_6^{Cl}$  ion was observed, corresponding to the only unique product detected for the chloridated oligosaccharide. Like maltoheptaose, the chloride-NA2 interaction appears to be weak as small increases in collision energy drastically reduced the abundance of the  $[M - H + Cl]^{2-}$  precursor ion.

### MS/MS of Chloridated Sialylated Oligosaccharides

EDD fragmentation patterns were examined for three chloride-adducted oligosaccharides containing one or two sialic acids. First studied was linear LS-tetrasaccharide, LSTa, with the following composition: Neu5Ac $\alpha$ 3Gal $\beta$ 3GlcNAc $\beta$ 3Gal $\beta$ 4GlcNAc. Next examined was LSTb, a similar LS-tetrasaccharide, exhibiting a branched structure due to the  $\alpha$ 2 $\rightarrow$ 6 linkage to galactose (Gal). A disialylacto-*N*-tetraose oligosaccharide (DSLNT) was also examined. With

a structure similar to LSTa, DSLNT contains an additional sialic acid residue that is  $\alpha$ 2 $\rightarrow$ 6 linked to GlcNAc.

CAD of all chloride-adducted sialylated oligosaccharides yielded little information, consistent with previous reports by Zaia et al. that sialylated carbohydrates require significantly more energy than neutral oligosaccharides for efficient fragmentation [8]. Energies sufficient to induce fragmentation of chloride-adducted sialylated oligosaccharides far exceeded the energy needed to dissociate the chloride-carbohydrate interaction, and the potential benefit of using this anion to stimulate alternative fragmentation pathways was thus lost. This shortcoming extols the benefit of alternative activation methods such as EDD for fragmentation of anion-adducted oligosaccharides.

For LSTa, a relatively abundant  $[M - H + Cl]^{2-}$  precursor ion was observed from standard negative ion mode electrospray ionization conditions. Following EDD of this precursor ion (Figure 3a), all resultant product ions were singly charged either by deprotonation or chloride adduction, with the exception of the peak at  $m/z=498.7$ . A  $Y_3$  fragment at  $m/z=543.2$  showed neutral hydrogen loss as the predominant species. Two C – 2H product ions,  $C_3 - 2H$  and  $C_4 - 2H$ , were observed, but unlike the neutral oligosaccharides discussed above, these products do not bear a chloride anion as the

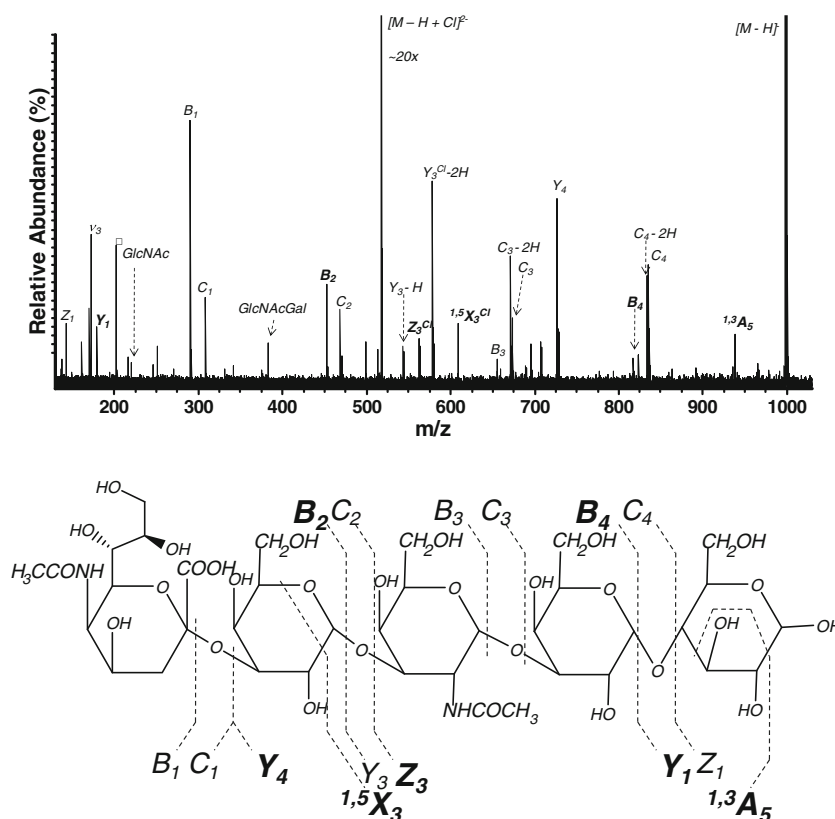


**Figure 3.** (Top) EDD product ion spectrum of deprotonated and chloride-adducted LSTa,  $[M - H + Cl]^{2-}$ , (50 scans, 2 s, bias voltage of  $-25$  V). Product ions shown in bold are unique to the chloride-adducted species compared to the corresponding doubly deprotonated species. Doubly charged product ions are indicated with an asterisk next to a product ion assignment. Squares indicate water loss from an adjacent product ion.  $v_3$  indicates the third harmonic. Superscript Cl indicates product ions bearing a chloride anion; (bottom) fragmentation pattern observed following EDD of deprotonated and chloride-adducted LSTa

charge carrier and were also observed following EDD of doubly deprotonated LSTa [30]. As stated previously, hydrogen abstraction products have been observed following heCAD in positive ion mode, but the precise mechanism generating such ions has not been elucidated [57]. Wolff et al. attempted to clarify this behavior in EDD of GAGs and proposed that electron detachment occurs at the carboxylate group of hexuronic acid, followed by hydrogen transfer to create an oxy radical at C2 or C3 and subsequently leading to the formation of a C - 2H product by  $\alpha$ -cleavage [32]. However, because we observe C - 2H species near the reducing end of the molecule (at C<sub>3</sub> and C<sub>4</sub>) it is unlikely that electron detachment

at the carboxylate group of sialic acid is responsible for these products. This seemingly unique behavior for the chloride-adducted precursor ion may be explained by the chloride adduct sharing a hydrogen with the sialic acid carboxylate group rather than with an oligosaccharide hydroxyl group (such carboxylic acid binding is not possible for maltoheptaose and NA2 as they lack sialic acid). This mode of binding, which prevents carboxylic acid deprotonation, was recently proposed by Cole and co-workers for chloride-peptide anionic complexes [66].

Glycosidic cleavage was detected between all monosaccharide units, and several fragments unique to the chloridated species were noted. These unique species include B<sub>2</sub>,

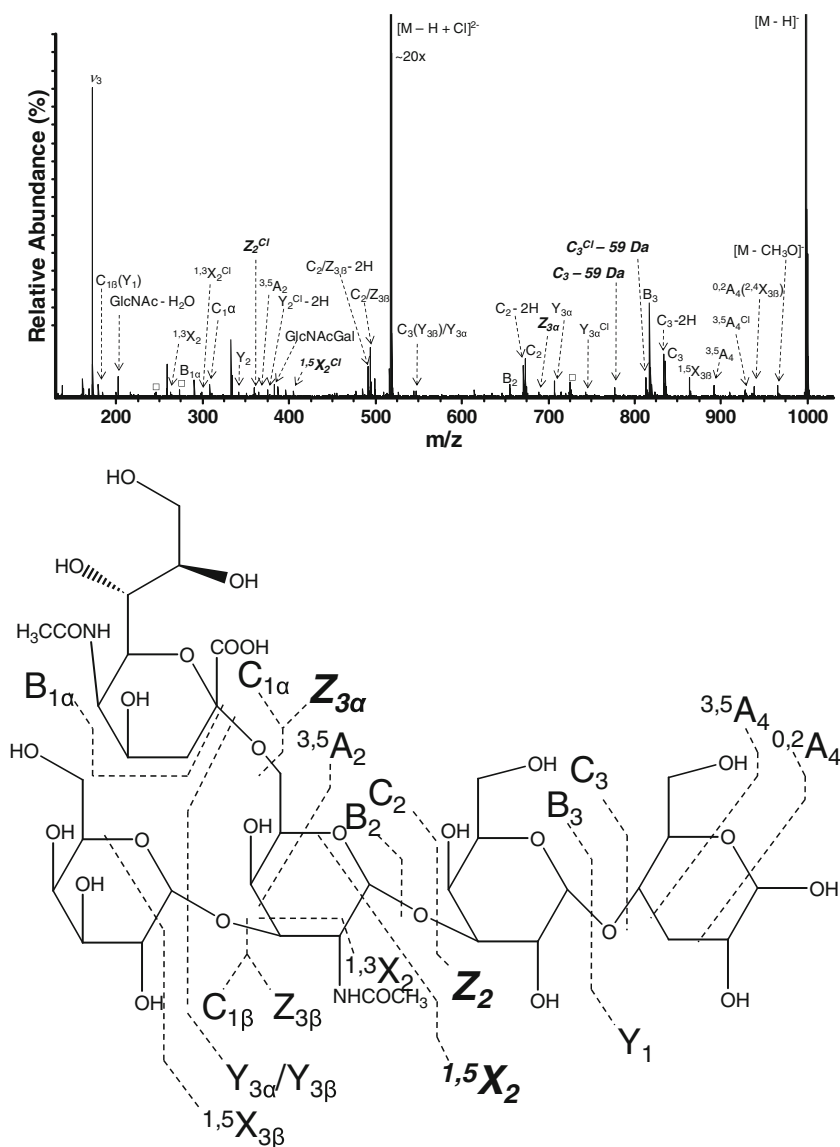


**Figure 4.** (Top) EDD of deprotonated and chloride-adducted LSTb,  $[M - H + Cl]^{2-}$ , (50 scans, 2 s, bias voltage of  $-35$  V). Product ions shown in bold are unique to the chloride-adducted species compared with the corresponding doubly deprotonated species. Doubly charged product ions are indicated with an asterisk next to a product ion assignment. Squares indicate water loss from an adjacent product ion. Ions due to multiple cleavage sites are designated with a slash between the sites of cleavage. Superscript Cl indicates product ions bearing a chloride anion. The branch containing sialic acid is referred to as the  $\alpha$ -branch in product ions labels; (bottom) fragmentation pattern observed following EDD of deprotonated and chloride-adducted LSTb



$B_4$ ,  $Y_1$ ,  $Y_4$ , and  $Z_3^{Cl}$  product ions. Unique cross-ring fragments include  $^{1,3}A_5$  and  $^{1,5}X_3^{Cl}$  ions. In previous experiments involving EDD of doubly deprotonated LSTa [30], cross-ring product ions were only observed following EDD, as opposed to vibrational excitation methods. Even though only two unique A and X-type fragments are observed in EDD of the chloride-adducted species, this finding represents a 2-fold increase in the number of cross-ring fragments detected compared to MS/MS of the doubly deprotonated species (Figure 3).

EDD of chloride-adducted LSTb showed extensive fragmentation, producing only singly charged product ions (Figure 4). Unique to the chloridated precursor ion are previously unobserved  $Z_2^{Cl}$ ,  $Z_{3\alpha}$ , as well as the cross-ring product  $^{1,5}X_2^{Cl}$ , which occurs at the branching GlcNAc

saccharide. The loss of  $CH_3O$  from the charge-reduced species has been detected following EDD of GAGs and is observed here at  $m/z=965.3$ . Several product ions resulting from multiple cleavage sites were noted, including  $C_2/Z_{3\beta}$ ,  $C_3(Y_{3\beta})/Y_{3\alpha}$ , GlcNAc –  $H_2O$ , and GlcNAcGal. The peak at  $m/z=614.2$ , denoted Neu5AcGal<sub>2</sub>, is believed to arise from saccharide rearrangement and has been detected in EDD of doubly deprotonated LSTb as well [30]. Carbohydrates have been shown to undergo saccharide rearrangement via internal residue loss during CAD [59, 67–69]. Unique to the chloridated oligosaccharide, peaks denoted as  $C_3 - 59$  Da and  $C_3^{Cl} - 59$  Da are believed to represent multiple cleavages that result in a  $C_3$  product ion that has lost  $C_2H_3O_2$ .

The chloride adduct of deprotonated disialylacto-*N*-tetraose oligosaccharide (DSLNT) was always of low

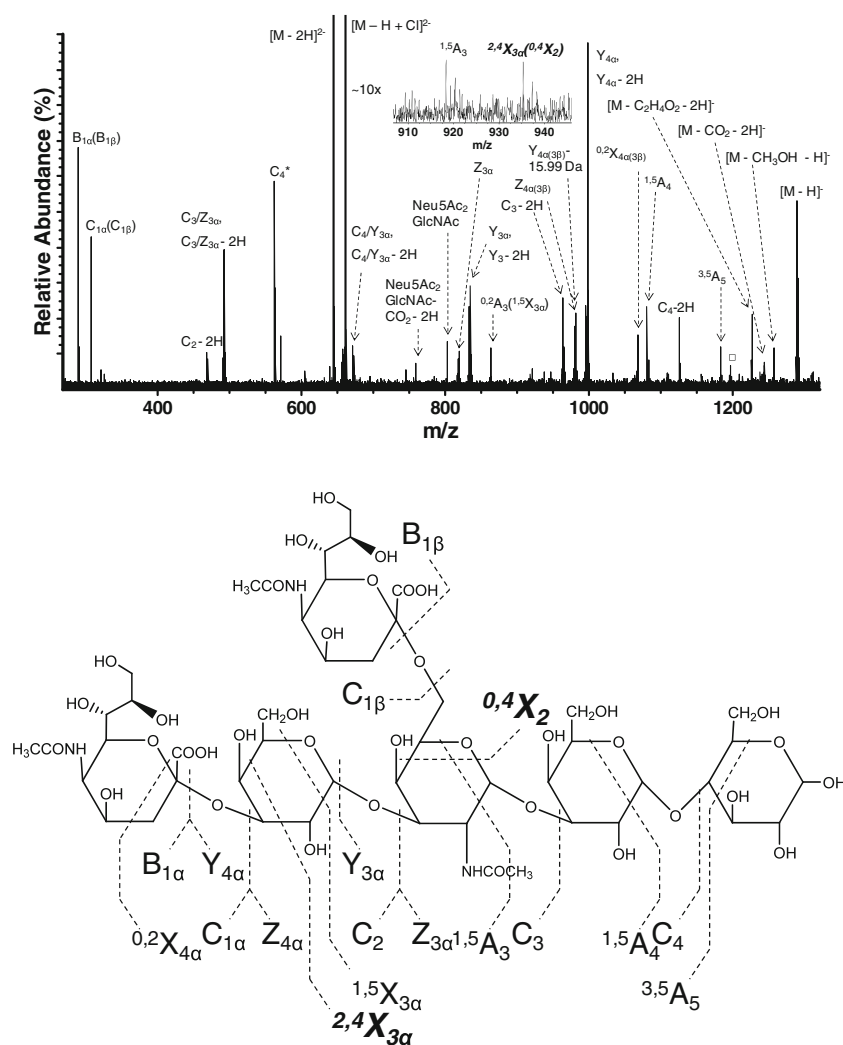


**Figure 5.** (Top) EDD of deprotonated and chloride-adducted DSLNT,  $[M - H + Cl]^{2-}$ , (50 scans, 2 s, bias voltage of  $-25$  V). Product ions shown in bold are unique to the chloride-adducted species compared with the corresponding doubly deprotonated species. Doubly charged product ions are indicated with an asterisk next to a product ion assignment. Squares indicate water loss from an adjacent product ion. Ions due to multiple cleavage sites are designated with a slash between the sites of cleavage. Superscript Cl indicates product ions bearing a chloride anion. The heavier branch containing sialic acid and galactose is referred to as the  $\alpha$ -branch in product ion labels; (bottom) fragmentation pattern observed following EDD of deprotonated and chloride-adducted DSLNT

abundance with respect to the doubly deprotonated ion following negative mode electrospray ionization. Two sialic acid residues makes DSLNT particularly amenable to EDD under standard conditions but makes isolation of the chloridated precursor ion particularly difficult due to ion suppression by the highly abundant doubly deprotonated species. The difficulty in precursor ion isolation could also be due to a higher lability of the chloride adduct due to the presence of one protonated sialic acid that can facilitate HCl loss. Attempts to isolate the chloridated precursor by quadrupole and in-cell isolation by CHEF [46] could not completely segregate the ion of interest from the doubly deprotonated species, and the  $[M - 2H]^{2-}$  ion remained at 75 % relative abundance under the best isolation conditions.

EDD of the semi-isolated chloride-adducted DSLNT showed fragmentation similar to that observed in previous experiments of the corresponding doubly deprotonated oligosaccharide, most likely resulting from the  $[M - 2H]^{2-}$  present at relatively high abundance in all experiments (Figure 5). Observed fragments arose from extensive backbone cleavage at all glycosidic bonds, and a number of cross-ring cleavages, resulting in  $^{1,5}A_4$ ,  $^{3,5}A_5$ ,  $^{1,5}X_{3\alpha}$ , and  $^{0,2}X_{4\alpha}$  ions, as well as a  $^{1,5}A_3$  ion, which occurs at a branching residue, were also detected. Several product ions resulting from neutral losses from the charge-reduced species were also noted, such as the relatively abundant peak designated  $[M - C_2H_4O_2 - 2H]^-$ . Even though no detected products contained a chloride adduct, the low abundance peak at  $m/z=935.3$ , denoted  $^{2,4}X_{3\alpha}({}^{0,4}X_2)$ , is unique to the chloridated sample. The low abundance of this unique ion suggests that adduction with a single chloride anion may not be compatible with EDD of oligosaccharides bearing two or more highly acidic protons.

## Conclusions

Our results demonstrate that EDD of underivatized chloride-adducted oligosaccharides provides structural information complementary to that from EDD of the corresponding doubly deprotonated species. EDD of chloridated oligosaccharides led to an increase in the types of cross-ring cleavages observed in all examples investigated, and generally showed an increase in the types of glycosidic fragments observed as well. Chloride adduction did not present a challenge for the formation of doubly charged anions for neutral oligosaccharides, but it remains a potential issue for acidic species. For neutral oligosaccharides, ion abundance of the  $[M - H + Cl]^{2-}$  precursor and doubly deprotonated anion were generally comparable and always considerably greater than the singly deprotonated species following electrospray ionization. The singly chloridated species was not observed with high abundance. Isolation of the chloride-adducted species for acidic oligosaccharides was challenging and generally required two stages of isolation (quadrupole and in-cell) due to the high abundance of the doubly deprotonated anion within close  $m/z$  proximity

to the chloridated precursor. Complete isolation of the doubly sialylated oligosaccharide (DSLNT) was not achieved and may be responsible for the lack of unique fragment ions observed in that case. Therefore, chloride adduction may not be appropriate for oligosaccharides bearing two or more acidic protons.

CAD experiments revealed a weak interaction between the carbohydrate and the chloride anion, which was easily displaced at low collision energies. However, CAD of neutral chloride-adducted oligosaccharides did produce unique cross-ring product ions not observed following EDD or CAD of doubly deprotonated samples, but cross-ring fragmentation was more extensive following EDD. Several unusual product ions resulting from abstraction of neutral hydrogen were observed in EDD of chloridated oligosaccharides, including  $C - H$ ,  $C - 2H$ , and  $Y - 2H$ , which have also been seen in EDD of doubly deprotonated species. The presence of a complementary product ion pair ( $C_3^{Cl} - 2H$  and  $Z_4^{Cl} + 2H$ ) in EDD of chloridated maltoheptaose further suggests that the previously noted  $Y - 16$  Da ions are actually  $Z + 2H$  ions. Due to the increase in glycosidic and cross-ring product ion formation, chloride adduction appears to be promising when used in conjunction with EDD for structural characterization of oligosaccharides. Future work includes improvement of sensitivity and throughput via (e.g., a more sensitive FT-ICR mass spectrometer [Solarix; Bruker Daltonics]) and use of nano-electrospray ionization. Chloride adduction should also be of interest in other alternative anion activation strategies for oligosaccharide structural characterization, including negative electron transfer dissociation [70] and 193 nm photodissociation [71].

## Acknowledgments

The authors acknowledge support for this work by an NSF Career Award, CHE 0547699 (to K.H.), a Smeaton Award for Undergraduate Summer Research (to J.R.K), and support by the University of Michigan.

## References

1. Varki, A.: Biological roles of oligosaccharides: All of the theories are correct. *Glycobiology* **3**, 97–130 (1993)
2. Dwek, R.A.: Glycobiology: Toward understanding the function of sugars. *Chem. Rev.* **96**, 683–720 (1996)
3. Parodi, A.J.: Protein glycosylation and its role in protein folding. *Annu. Rev. Biochem.* **69**, 60–93 (2000)
4. Rudd, P.M., Elliott, T., Cresswell, P., Wilson, I.A., Dwek, R.A.: Glycosylation and the immune system. *Science* **291**, 2370–2376 (2001)
5. Harvey, D.J.: Matrix-assisted laser desorption/ionization mass spectrometry of carbohydrates. *Mass Spectrom. Rev.* **18**, 349–451 (1999)
6. Zaia, J.: Mass spectrometry of oligosaccharides. *Mass Spectrom. Rev.* **23**, 161–227 (2004)
7. Park, Y., Lebrilla, C.B.: Application of fourier transform ion cyclotron resonance mass spectrometry to oligosaccharides. *Mass Spectrom. Rev.* **24**, 232–264 (2005)
8. Seymour, J.L., Costello, C.E., Zaia, J.: The influence of sialylation on glycan negative ion dissociation and energetics. *J. Am. Soc. Mass Spectrom.* **17**, 844–854 (2006)

9. Zhou, Z., Ogden, S., Leary, J.A.: Linkage position determination in oligosaccharides: MS/MS study of lithium-cationized carbohydrates. *J. Org. Chem.* **55**, 5446–5448 (1990)
10. Orlando, R., Bush, C.A., Fenselau, C.: Structural analysis of oligosaccharides by tandem mass spectrometry: Collisional activation of sodium adduct ions. *Biomed. Environ. Mass Spectrom.* **19**, 747–754 (1990)
11. Fura, A., Leary, J.A.: Differentiation of Ca<sup>2+</sup>- and Mg<sup>2+</sup>-coordinated branched trisaccharide isomers: An electrospray ionization and tandem mass spectrometry study. *Anal. Chem.* **65**, 2805–2811 (1993)
12. Cancilla, M.T., Penn, S.G., Carroll, J.A., Lebrilla, C.B.: Coordination of alkali metals to oligosaccharides dictates fragmentation behavior in matrix assisted laser desorption ionization fourier transform mass spectrometry. *J. Am. Chem. Soc.* **118**, 6736–6745 (1996)
13. Adamson, J.T., Håkansson, K.: Electron capture dissociation of oligosaccharides ionized with alkali, alkaline earth, and transition metals. *Anal. Chem.* **79**, 2901–2910 (2007)
14. Zubarev, R.A., Kelleher, N.L., McLafferty, F.W.: Electron capture dissociation of multiply charged protein cations. A nonergodic process. *J. Am. Chem. Soc.* **120**, 3265–3266 (1998)
15. Zubarev, R.A., Kruger, N.A., Fridriksson, E.K., Lewis, M.A., Horn, D.M., Carpenter, B.K., McLafferty, F.W.: Electron capture dissociation of gaseous multiply-charged proteins is favored at disulfide bonds and other sites of high hydrogen atom affinity. *J. Am. Chem. Soc.* **121**, 2857–2862 (1999)
16. Zhao, C., Xie, B., Chan, S.Y., Costello, C.E., O'Connor, P.B.: Collisionally activated dissociation and electron capture dissociation provide complementary structural information for branched permethylated oligosaccharides. *J. Am. Soc. Mass Spectrom.* **19**, 138–150 (2008)
17. Cooper, H.J., Håkansson, K., Marshall, A.G.: The role of electron capture dissociation in biomolecular analysis. *Mass Spectrom. Rev.* **24**, 201–222 (2005)
18. Mirgorodskaya, E., Roepstorff, P., Zubarev, R.A.: Localization of O-glycosylation sites in peptides by electron capture dissociation in a fourier transform mass spectrometer. *Anal. Chem.* **71**, 4431–4436 (1999)
19. Håkansson, K., Cooper, H.J., Emmett, M.R., Costello, C.E., Marshall, A.G., Nilsson, C.L.: Electron capture dissociation and infrared multiphoton dissociation MS/MS of an N-glycosylated tryptic peptide yield complementary sequence information. *Anal. Chem.* **73**, 4530–4536 (2001)
20. Kjeldsen, F., Haselmann, K.F., Budnik, B.A., Sorensen, E.S., Zubarev, R.A.: Complete characterization of posttranslational modification sites in the bovine milk protein pp3 by tandem mass spectrometry with electron capture dissociation as the last stage. *Anal. Chem.* **75**, 2355–2361 (2003)
21. Håkansson, K., Chalmers, M.J., Quinn, J.P., McFarland, M.A., Hendrickson, C.L., Marshall, A.G.: Combined electron capture and infrared multiphoton dissociation for multistage MS/MS in an FT-ICR mass spectrometer. *Anal. Chem.* **75**, 3256–3262 (2003)
22. Mormann, M., Macek, B., de Peredo, A.G., Hofsteenge, J., Peter-Katalinic, J.: Structural studies on protein O-fucosylation by electron capture dissociation. *Int. J. Mass Spectrom.* **234**, 11–21 (2004)
23. Adamson, J.T., Håkansson, K.: Infrared multiphoton dissociation and electron capture dissociation of high-mannose type glycopeptides. *J. Proteome Res.* **5**, 493–501 (2006)
24. Han, L., Costello, C.E.: Electron transfer dissociation of milk oligosaccharides. *J. Am. Soc. Mass Spectrom.* **22**, 997–1013 (2011)
25. Dallinga, J., Heerma, W.: Reaction mechanism and fragment ion structure determination of deprotonated small oligosaccharides, studied by negative ion fast atom bombardment (Tandem) mass spectrometry. *Biol. Mass Spectrom.* **20**, 215–231 (1991)
26. Li, D.T., Her, G.R.: Linkage analysis of chromophore-labeled disaccharides and linear oligosaccharides by negative ion fast atom bombardment ionization and collisional-induced dissociation with B/E scanning. *Anal. Biochem.* **211**, 250–257 (1993)
27. Carroll, J.A., Ngoka, L.C., Beggs, C.G., Lebrilla, C.B.: Liquid secondary ion mass spectrometry/fourier transform mass spectrometry of oligosaccharide anions. *Anal. Chem.* **65**, 1582–1587 (1993)
28. Chai, W., Piskarev, V., Lawson, A.M.: Negative-ion electrospray mass spectrometry of neutral underivatized oligosaccharides. *Anal. Chem.* **73**, 651–657 (2001)
29. Domon, B., Costello, C.E.: A systematic nomenclature for carbohydrate fragmentations in FAB-MS/MS spectra of glycoconjugates. *Glycoconj. J.* **5**, 397–409 (1988)
30. Adamson, J.T., Håkansson, K.: Electron detachment dissociation of neutral and sialylated oligosaccharides. *J. Am. Soc. Mass Spectrom.* **18**, 2162–2172 (2007)
31. Wolff, J.J., Amster, I.J., Chi, L., Linhardt, R.J.: Electron detachment dissociation of glycosaminoglycan tetrasaccharides. *J. Am. Soc. Mass Spectrom.* **18**, 234–244 (2007)
32. Wolff, J.J., Chi, L., Linhardt, R.J., Amster, I.J.: Distinguishing glucuronic from iduronic acid in glycosaminoglycan tetrasaccharides by using electron detachment dissociation. *Anal. Chem.* **79**, 2015–2022 (2007)
33. Wolff, J.J., Laremore, T.N., Busch, A.M., Linhardt, R.J., Amster, I.J.: Electron detachment dissociation of dermatan sulfate oligosaccharides. *J. Am. Soc. Mass Spectrom.* **19**, 294–304 (2008)
34. Budnik, B.A., Haselmann, K.F., Zubarev, R.A.: Electron detachment dissociation of peptide dianions: An electron-hole recombination phenomenon. *Chem. Phys. Lett.* **342**, 299–302 (2001)
35. Kjeldsen, F., Silivra, O.A., Ivonin, I.A., Haselmann, K.F., Gorshkov, M., Zubarev, R.A.: C- $\alpha$ -C Backbone fragmentation dominates in electron detachment dissociation of gas-phase polypeptide polyanions. *Chem. Eur. J.* **11**, 1803–1812 (2005)
36. Kalli, A., Håkansson, K.: Preferential cleavage of SOS and COS bonds in electron detachment dissociation and infrared multiphoton dissociation of disulfide-linked peptide anions. *Int. J. Mass Spectrom.* **263**, 71–81 (2007)
37. Kweon, H.K., Håkansson, K.: Metal oxide-based enrichment combined with gas-phase ion-electron reactions for improved mass spectrometric characterization of protein phosphorylation. *J. Proteome Res.* **7**, 749–755 (2008)
38. Yang, J., Mo, J., Adamson, J.T., Håkansson, K.: Characterization of oligonucleotides by electron detachment dissociation fourier transform ion cyclotron resonance mass spectrometry. *Anal. Chem.* **77**, 1876–1882 (2005)
39. Mo, J.J., Håkansson, K.: Characterization of nucleic acid higher order structure by high-resolution tandem mass spectrometry. *Anal. Bioanal. Chem.* **386**, 675–681 (2006)
40. McFarland, M.A., Marshall, A.G., Hendrickson, C.L., Nilsson, C.L., Fredman, P., Mansson, J.E.: Structural characterization of the GM1 ganglioside by infrared multiphoton dissociation/electron capture dissociation, and electron detachment dissociation electrospray ionization FT-ICR MS/MS. *J. Am. Soc. Mass Spectrom.* **16**, 752–762 (2005)
41. Wong, A.W., Cancilla, M.T., Voss, L.R., Lebrilla, C.B.: Anion dopant for oligosaccharides in matrix-assisted laser desorption/ionization mass spectrometry. *Anal. Chem.* **71**, 205–211 (1999)
42. Harvey, D.J.: Fragmentation of negative ions from carbohydrates: Part 1. Use of nitrate and other anionic adducts for the production of negative ion electrospray spectra from N-linked carbohydrates. *J. Am. Soc. Mass Spectrom.* **16**, 622–630 (2005)
43. Guan, B., Cole, R.B.: MALDI linear-field reflectron TOF post-source decay analysis of underivatized oligosaccharides: Determination of glycosidic linkages and anomeric configurations using anion attachment. *J. Am. Soc. Mass Spectrom.* **19**, 1119–1131 (2008)
44. Yang, J., Håkansson, K.: Characterization and optimization of electron detachment dissociation fourier transform ion cyclotron resonance mass spectrometry. *Int. J. Mass Spectrom.* **276**, 144–148 (2008)
45. Caravatti, P., Allemann, M.: The infinity cell—a new trapped ion cell with radiofrequency covered trapping electrodes for fourier transform ion cyclotron resonance mass spectrometry. *Org. Mass Spectrom.* **26**, 514–518 (1991)
46. Heck, A.J.R., Derrick, P.J.: Ultrahigh mass accuracy in isotope selective collision-induced dissociation using correlated sweep excitation and sustained off-resonance irradiation: A fourier transform mass spectrometry case study on the  $[M+2H]^{2+}$  ion of bradykinin. *Anal. Chem.* **69**, 3603–3607 (1997)
47. Tsybin, Y.O., Witt, M., Baykut, G., Kjeldsen, F., Håkansson, P.: Combined infrared multiphoton dissociation and electron capture dissociation with a hollow electron beam in fourier transform ion cyclotron resonance mass spectrometry. *Rapid Commun. Mass Spectrom.* **17**, 1759–1768 (2003)
48. Senko, M.W., Canterbury, J.D., Guan, S., Marshall, A.G.: A high performance modular data system for FT-ICR mass spectrometry. *Rapid Commun. Mass Spectrom.* **10**, 1839–1844 (1996)
49. Lohmann, K.K., von der Lieth, C.W.: GlycoFragment and GlycoSearchMS: Web tools to support the interpretation of mass

- spectra of complex carbohydrates. *Nucleic Acids Res.* **32**, 261–266 (2004)
50. Berry, R.S.: Small free negative ions. *Chem. Rev.* **69**, 533–542 (1969)
51. Alconcel, L.S., Deyerl, H.-J., DeClue, M., Continetti, R.E.: Dissociation dynamics and stability of cyclic alkoxy radicals and alkoxide anions. *J. Am. Chem. Soc.* **123**, 3125–3132 (2001)
52. Harvey, D.J., Bateman, R.H., Green, B.N.: High-energy collision-induced fragmentation of complex oligosaccharides ionized by matrix-assisted laser desorption/ionization mass spectrometry. *J. Mass Spectrom.* **32**, 167–187 (1997)
53. Küster, B., Naven, T.J.P., Harvey, D.J.: Effect of the reducing-terminal substituents on the high energy collision-induced dissociation matrix-assisted laser desorption/ionization mass spectra of oligosaccharides. *Rapid Commun. Mass Spectrom.* **10**, 1645–1651 (1996)
54. Stephens, E., Maslen, S.L., Green, L.G., Williams, D.H.: Fragmentation characteristics of neutral-N-linked glycans using a MALDI-TOF/TOF tandem mass spectrometer. *Anal. Chem.* **76**, 2343–2354 (2004)
55. Lewandrowski, U., Resemann, A., Sickmann, A.: Laser-induced dissociation/high-energy collision-induced dissociation fragmentation using MALDI-TOF/TOF-MS instrumentation for the analysis of neutral and acidic oligosaccharides. *Anal. Chem.* **77**, 3274–3283 (2005)
56. Yu, S., Wu, S., Khoo, K.: Distinctive characteristics of MALDI-Q/TOF and TOF/TOF tandem mass spectrometry for sequencing of permethylated complex type N-glycans. *Glyconj. J.* **23**, 355–369 (2006)
57. Kováčik, V., Hirsch, J., Kovac, P., Heerma, W., Thomas-Oates, J., Haverkamp, J.: Oligosaccharide characterization using collision-induced dissociation fast atom bombardment mass spectrometry: Evidence for internal monosaccharide residue loss. *J. Mass Spectrom.* **30**, 949–958 (1995)
58. Savitski, M.M., Kjeldsen, F., Nielsen, M.L., Zubarev, R.A.: Hydrogen rearrangement to and from radical z fragments in electron capture dissociation of peptides. *J. Am. Soc. Mass Spectrom.* **18**, 113–120 (2006)
59. O'Connor, P.B., Lin, C., Courmoyer, J.J., Pittman, J.L., Belyayev, M., Budnik, B.A.: Long-lived electron capture dissociation product ions experience radical migration via hydrogen abstraction. *J. Am. Soc. Mass Spectrom.* **17**, 576–585 (2006)
60. Harvey, D.J.: Fragmentation of negative ions from carbohydrates. Part 2. Fragmentation of high-mannose N-linked glycans. *J. Am. Soc. Mass Spectrom.* **16**, 631–646 (2005)
61. Harvey, D.J.: Fragmentation of negative ions from carbohydrates: Part 3. Fragmentation of hybrid and complex N-linked glycans. *J. Am. Soc. Mass Spectrom.* **16**, 647–659 (2005)
62. Dell, A.F.A.B.: Mass spectrometry of carbohydrates. *Adv. Carbohydr. Chem. Biochem.* **45**, 19–72 (1987)
63. Spengler, B., Dolce, J.W., Cotter, R.J.: Infrared-laser desorption mass spectrometry of oligosaccharides – fragmentation mechanisms and isomer analysis. *Anal. Chem.* **62**, 1731–1737 (1990)
64. Carroll, J., Willard, D., Lebrilla, C.: Energetics of cross-ring cleavages and their relevance to the linkage determination of oligosaccharides. *Anal. Chim. Acta* **307**, 431–447 (1995)
65. Saad, O.M., Leary, J.A.: Delineating mechanisms of dissociation for isomeric heparin disaccharides using isotope labeling and ion trap tandem mass spectrometry. *J. Am. Soc. Mass Spectrom.* **15**, 1274–1286 (2004)
66. Liu, X.H., Cole, R.B.: A new model for multiply charged adduct formation between peptides and anions in electrospray mass spectrometry. *J. Am. Soc. Mass Spectrom.* **22**, 2125–2136 (2011)
67. Ernst, B., Müller, R.T., Richter, W.J.: False sugar sequence ions in electrospray tandem mass spectrometry of underivatized sialyl-lewis-type oligosaccharides. *Int. J. Mass. Spectrom. Ion Process.* **160**, 283–290 (1997)
68. Brüll, L.P., Heerma, W., Thomas-Oates, J., Haverkamp, J., Kováčik, V., Kovác, P.: Loss of internal 1<sub>6</sub> substituted monosaccharide residues from underivatized and per-O-methylated trisaccharides. *J. Am. Soc. Mass Spectrom.* **8**, 43–49 (1997)
69. Harvey, D.J., Mattu, T.S., Wormald, M.R., Royle, L., Dwek, R.A., Rudd, P.M.: “Internal residue loss”; Rearrangements occurring during the fragmentation of carbohydrates derivatized at the reducing terminus. *Anal. Chem.* **74**, 734–740 (2002)
70. Wolff, J.J., Leach, F.E., Laremore, T.N., Kaplan, D.A., Easterling, M.L., Linhardt, R.J., Amster, I.J.: Negative electron transfer dissociation of glycosaminoglycans. *Anal. Chem.* **82**, 3460–3466 (2010)
71. Ko, B.J., Brodbelt, J.S.: 193 nm ultraviolet photodissociation of deprotonated sialylated oligosaccharides. *Anal. Chem.* **83**, 8192–8200 (2011)